

Regular Article

## Development of Radon and Thoron Exposure Systems at Hirosaki University

Chanis Pornnumpa<sup>1,†</sup>, Yui Oyama<sup>2</sup>, Kazuki Iwaoka<sup>1</sup>,  
Masahiro Hosoda<sup>3</sup> and Shinji Tokonami<sup>1\*</sup>

<sup>1</sup>Hirosaki University, Institute of Radiation Emergency Medicine, 66-1 Hon-cho, Hirosaki, Aomori 036-8564, Japan

<sup>2</sup>Hirosaki University, School of Health Sciences, 66-1 Hon-cho, Hirosaki, Aomori 036-8564, Japan

<sup>3</sup>Hirosaki University Graduate School of Health Sciences, 66-1 Hon-cho, Hirosaki, Aomori 036-8564, Japan

<sup>†</sup>Present address: Kasetsart University, Faculty of Sciences, Department of Applied Radiation and Isotope, 50 Ngam Wong Wan Rd., Lat Yao, Chatuchak, Bangkok, Thailand

Received 22 May 2017; revised 25 July 2017; accepted 27 December 2017

Radon ( $^{222}\text{Rn}$ ) and thoron ( $^{220}\text{Rn}$ ) exposure systems were designed and developed for calibrating radioactive gas monitors, based on the quality assurance (QA) and quality control (QC) standards of the monitors at Hirosaki University, Japan. To monitor the concentration levels of radioactive gases, gas monitors were installed inside an exposure chamber together with a temperature-humidity meter for recording inside and outside conditions during performance tests. In this study, radioactive gases generated from natural rock were used as the  $^{222}\text{Rn}$  source and commercial lantern mantles enriched with thorium ( $^{232}\text{Th}$ ) were used as the  $^{220}\text{Rn}$  source. The concentration levels were kept within a range between 0.2 and 10 kBq m<sup>-3</sup> for the  $^{222}\text{Rn}$  exposure system and between 3.5 and 29 kBq m<sup>-3</sup> for the  $^{220}\text{Rn}$  exposure system. The results obtained demonstrated that the concentration levels depended on such factors as the type of sources, flow rates of the radioactive gases generated into the chamber, gases emanating from the sources, and humidity in the gas generation system, and they are described in the paper. However, performance tests of these exposure systems were carried out and their results showed that  $^{222}\text{Rn}$  and  $^{220}\text{Rn}$  concentrations in the exposure chamber could be easily controlled through manually setting the flow rate and relative humidity and the distribution of gases was fairly homogenous.

*Key words:* exposure chamber, radon chamber, thoron chamber, calibration chamber

### 1. Introduction

Radon ( $^{222}\text{Rn}$ ), thoron ( $^{220}\text{Rn}$ ), and their progeny are important sources of ionizing radiation and ionizing radiation is an important factor affecting human

health from the viewpoint of radiation exposure. Environmental exposure caused by radioactive gases is a significant cause of internal exposure when air containing radioactive materials is inhaled into the body via the respiratory tract<sup>1-3</sup>. Short-lived decay products of  $^{222}\text{Rn}$  ( $^{218}\text{Po}$ ,  $^{214}\text{Po}$  and  $^{214}\text{Bi}$ ) and  $^{220}\text{Rn}$  ( $^{212}\text{Po}$ ) which emit alpha or beta radiation can be considered as dangerous radionuclides that can interact with biological tissues in the lung as the alpha or beta particles move through the cells, and this interaction can lead to cancer and DNA damage. Additionally,  $^{222}\text{Rn}$

\*Shinji Tokonami: Department of Radiation Physics, Institute of Radiation Emergency Medicine, Hirosaki University, 66-1 Hon-cho, Hirosaki, Aomori 036-8564, Japan  
E-mail: tokonami@hirosaki-u.ac.jp

has been mentioned to be the second most common cause of lung cancer after smoking for the general population<sup>1</sup>. In the United States, more than 20,000 people die each year from lung cancer caused by indoor  $^{222}\text{Rn}$  exposure<sup>4</sup>. The United States Environmental Protection Agency (USEPA)<sup>4</sup> has found that smokers who live in areas where indoor  $^{222}\text{Rn}$  levels are high, have increased risk of lung cancer from inhalation.

Even though  $^{220}\text{Rn}$  is less dangerous than  $^{222}\text{Rn}$  because of its shorter half-life, many indoor  $^{220}\text{Rn}$  surveys in Europe and Asia have revealed that the amount of  $^{220}\text{Rn}$  and its progeny inhaled through the air can be equal to or even exceed that of  $^{222}\text{Rn}$  and its progeny<sup>5-10</sup>. In some areas where  $^{232}\text{Th}$ -rich building materials are used or in high background radiation areas (HBRAs),  $^{220}\text{Rn}$  may represent a significant source of radioactive exposure. Therefore, measuring techniques and dose conversion factors (DCFs) have been developed to measure the  $^{220}\text{Rn}$  progeny exposure level<sup>7-10</sup>.

Radiation exposure chambers have been developed to accurately evaluate radiation instruments and key procedures in laboratories. In Japan, the National Institute of Radiological Sciences (NIRS) has developed  $^{222}\text{Rn}$  and  $^{220}\text{Rn}$  chambers that can be used for calibration, evaluation and inter-comparison purposes<sup>11-13</sup>. The main  $^{222}\text{Rn}$  chamber with an inner volume of 24.45 m<sup>3</sup> and a 150 L stainless steel  $^{220}\text{Rn}$  chamber have been used for working with radioactive gases and their progeny.

Sorimachi *et al.*<sup>13</sup> studied generation methods and control of  $^{220}\text{Rn}$  emanated from lantern mantles by using the rate of air flow in the experimental chamber at NIRS, and found that the concentration of  $^{220}\text{Rn}$  generated in the air ranged from 0.9 to 150 kBq m<sup>-3</sup> and it exponentially depended on the absolute humidity (AH). The generation methods and control approach of Sorimachi *et al.* was applied to develop a  $^{220}\text{Rn}$  exposure system at Hirosaki University.

Similar experiments have also been carried out in other countries. In Syria, tests to calibrate a  $^{222}\text{Rn}$  chamber were carried out by Shweikini *et al.*<sup>14</sup> using a solid  $^{226}\text{Ra}$  source with an activity of 122 kBq, where the  $^{222}\text{Rn}$  activity concentration was determined to be 170 kBq m<sup>-3</sup> by solid state nuclear track detectors (SSNTDs). In Kuwait, Al-Azmi<sup>15</sup> used a  $^{222}\text{Rn}$  source from soil in a cylindrical stainless steel container with a volume of 101 L for calibrating  $^{222}\text{Rn}$  measuring devices. The concentration obtained was estimated to be between 172-501 Bq m<sup>-3</sup>, where reservoirs with different volumes of 5, 10, and 20 L were filled with soil gas<sup>11</sup>. Zhao *et al.*<sup>5</sup> designed a simple  $^{220}\text{Rn}$  chamber using commercial lantern mantles enriched for generating  $^{220}\text{Rn}$  gas. The concentration level generated was between 0.5 to 80 kBq m<sup>-3</sup>. Furthermore, Abdalla and Al-Hajry<sup>16</sup> designed and constructed an irradiation  $^{222}\text{Rn}$  chamber using soil as a  $^{222}\text{Rn}$  source. The

average specific activity of radium in the soil sample was estimated to be  $182 \pm 13$  Bq kg<sup>-1</sup>. As more dose assessments of  $^{220}\text{Rn}$  exposure to humans are being made, a  $^{220}\text{Rn}$  calibration system has been established and designed to support  $^{220}\text{Rn}$  measuring devices in this study.

Surveys to measure  $^{222}\text{Rn}$ ,  $^{220}\text{Rn}$ , and their progenies have been conducted in several HBRAs around the world, especially at locations where there is an accumulation of radioactive gases or a suspected accumulation. Many measurement techniques are used for monitoring  $^{222}\text{Rn}$  and  $^{220}\text{Rn}$  in the environment, and it is necessary to provide calibration facilities to calibrate the monitoring devices<sup>14, 15, 17</sup>. In Japan, there are not enough radiation instruments calibration facilities to accommodate the increasing need for radiation monitoring. To support internal dose assessment and radiological instrument calibration, including methods for testing radioactive gases and their progeny, two  $^{222}\text{Rn}$  and  $^{220}\text{Rn}$  exposure systems were designed and developed in this study. Then performance tests were carried out to determine the calibration factor of the radioactive gas monitors, stability of radioactivity concentrations, and their levels.

## 2. Materials and methods

### 2.1. Structure of $^{222}\text{Rn}$ exposure system

The exposure chamber is made of a stainless-steel cylinder. The top of the chamber is locked by a stainless-steel O-ring lock system between the lid and the tank body. Inside the tank, a fan is installed on the upper-side to provide a uniform stability for the radioactive gases. For the  $^{222}\text{Rn}$  exposure system, some amount of natural uranium ore is placed inside an acrylic container (volume of 6.76 L), which  $^{222}\text{Rn}$  gas by natural radioactive decay. Activity of the source was not directly measured. However, the contribution of thoron from the uranium ore was investigated using 18 passive integrating  $^{222}\text{Rn}$ - $^{220}\text{Rn}$  discriminative monitors (Raduet, Radosys, Ltd., Hungary) in the chamber, and the  $^{220}\text{Rn}$  concentration level was below the limit that the monitors could measure.

Before operating the system, the concentration level was controlled by the  $^{222}\text{Rn}$  gas emission time. For the  $^{222}\text{Rn}$  gas preparation process, the  $^{222}\text{Rn}$  concentration level from the uranium ore had to be reset before starting as  $^{222}\text{Rn}$  gas can accumulate in the container by release from the source.  $^{222}\text{Rn}$  gas accumulated in the container was eliminated by evacuating the gas using a pump and waiting one day to stabilize the radioactive gas production level. The stability of  $^{222}\text{Rn}$  gas production was tested 10 times using  $^{222}\text{Rn}$  gas injection. During all experiments, the temperature of the system was controlled by the laboratory air conditioning system to be between 20 and 22°C. The  $^{222}\text{Rn}$  exposure was done by two methods: spot-

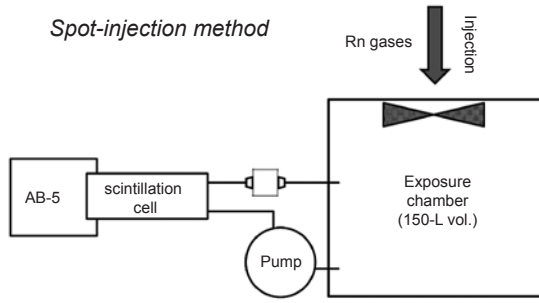


Fig. 1. Layout of <sup>222</sup>Rn exposure system: spot-injection method.

Table 1. The conversion factors for <sup>222</sup>Rn concentration calculation in spot-injection method

Time interval in hours	$\overline{CF}$ (Bq m <sup>-3</sup> cpm <sup>-1</sup> ) <sup>a</sup>
0 – 1	41.5
1 – 2	31.3
2 – 3	28.8
3 – 4	28.4
> 4	28.4

<sup>a</sup> $\overline{CF}$  is defined as a time interval during measurements

Table 2. All parameters for the conversion factor calculation

Nuclides	Decay mode	Concentration at initial phase; C <sub>0</sub> (Bq)	Half-life <sup>(21)</sup>	Decay constant (s <sup>-1</sup> )	Alpha counting efficiency (cpm) <sup>(18)</sup>
<sup>222</sup> Rn	<i>a</i>	1	3.8 d	2.10 × 10 <sup>-6</sup>	0.63
<sup>218</sup> Po	<i>a</i>	0	3.1 min	3.73 × 10 <sup>-3</sup>	0.74
<sup>214</sup> Pb	<i>β</i>	0	26.8 min	4.31 × 10 <sup>-4</sup>	-
<sup>214</sup> Bi	<i>β</i>	0	19.9 min	5.81 × 10 <sup>-4</sup>	-
<sup>214</sup> Po	<i>a</i>	0	1.6 × 10 <sup>-4</sup> s	4.22 × 10 <sup>-3</sup>	0.86

injection and Once-through methods that are described in the next section.

### 2.1.1. Spot-injection method

Figure 1 shows the layout of the exposure system. Three volumes of <sup>222</sup>Rn gas (1,000 mL, 3,000 mL, and 5,000 mL) were injected into a 150 L exposure chamber and were utilized for studying the characteristics of <sup>222</sup>Rn and their decay constants for around 120 hours to evaluate the initial activity in each condition and the magnitude of chamber leakage tests. During the operation, a portable radiation monitor (AB-5, Pylon Electronics Inc., Canada) with a scintillation cell (300A, Pylon Electronics Inc.) was used to measure the counts of the concentration level every 1 hour and values were converted to Bq m<sup>-3</sup> by the conversion factor (*CF*). The *CF* values used for the <sup>222</sup>Rn concentration calculation in the range of the delay time of the scintillation cell (3.5 hours after starting measurement) are shown in Table 1; they have been explained by Tokonami *et al*<sup>(18)</sup>. The parameters for alpha counting efficiency calculation of the scintillation cell by a Monte Carlo method were used for estimating the *CF* value according to equation (1).

$$CF = \frac{1}{(A_1 \eta_{Rn-222} + A_2 \eta_{Po-218} + A_3 \eta_{Po-214}) \times V \times 60} \quad (1)$$

When *CF* is conversion factor of <sup>222</sup>Rn concentration (Bq m<sup>-3</sup> cpm<sup>-1</sup>). *A*<sub>1</sub>, *A*<sub>2</sub>, and *A*<sub>3</sub> are activity concentrations (Bq m<sup>-3</sup>) of <sup>222</sup>Rn, <sup>218</sup>Po, and <sup>214</sup>Po as time elapsed, which is estimated by equations (2)-(4).  $\eta_{Rn}$ ,  $\eta_{Po-218}$ , and  $\eta_{Po-214}$  are alpha counting efficiencies obtained by a Monte

Carlo calculation. *V* is inner volume of cell in unit of m<sup>3</sup> (0.00027 m<sup>3</sup>). The parameters are shown in Table 2.

$$A_1 = C_0 e^{-\lambda_{Rn-222} t} \quad (2)$$

$$A_2 = \left( \frac{C_0 \lambda_{Po-218}}{\lambda_{Po-218} - \lambda_{Rn-222}} \right) \times \left[ \left( e^{-\lambda_{Rn-222} t} \right) - \left( e^{-\lambda_{Po-218} t} \right) \right] \quad (3)$$

$$A_3 = 0.99978 \times 0.99979 C_0 \lambda_{Po-218} \lambda_{Pb-214} \lambda_{Bi-214} \lambda_{Po-214} \times \left[ \frac{e^{-\lambda_{Rn-222} t}}{\lambda_a} \right] + \left[ \frac{e^{-\lambda_{Po-218} t}}{\lambda_b} \right] + \left[ \frac{e^{-\lambda_{Pb-214} t}}{\lambda_c} \right] + \left[ \frac{e^{-\lambda_{Bi-214} t}}{\lambda_d} \right] + \left[ \frac{e^{-\lambda_{Po-214} t}}{\lambda_e} \right] \quad (4)$$

Here, *C*<sub>0</sub> (Bq) is concentration at initial phase. Decay constants  $\lambda$  (s<sup>-1</sup>) of each nuclide are shown in the Table 2.  $\lambda_a$  to  $\lambda_e$  (s<sup>-1</sup>) are described by equations (5)-(9). *t* (s) is time after *t* = 0.

$$\lambda_a = (\lambda_{Po-218} - \lambda_{Rn-222}) \times (\lambda_{Pb-214} - \lambda_{Rn-222}) \times (\lambda_{Bi-214} - \lambda_{Rn-222}) \times (\lambda_{Po-214} - \lambda_{Rn-222}) \quad (5)$$

$$\lambda_b = (\lambda_{Rn-222} - \lambda_{Po-218}) \times (\lambda_{Pb-214} - \lambda_{Po-218}) \times (\lambda_{Bi-214} - \lambda_{Po-218}) \times (\lambda_{Po-214} - \lambda_{Po-218}) \quad (6)$$

$$\lambda_c = (\lambda_{Rn-222} - \lambda_{Pb-214}) \times (\lambda_{Po-218} - \lambda_{Pb-214}) \times (\lambda_{Bi-214} - \lambda_{Pb-214}) \times (\lambda_{Po-214} - \lambda_{Pb-214}) \quad (7)$$

$$\lambda_d = (\lambda_{Rn-222} - \lambda_{Bi-214}) \times (\lambda_{Po-218} - \lambda_{Bi-214}) \times (\lambda_{Pb-214} - \lambda_{Bi-214}) \times (\lambda_{Po-214} - \lambda_{Bi-214}) \quad (8)$$

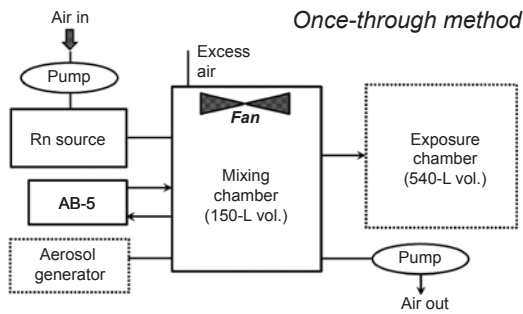


Fig. 2. Layout of  $^{222}\text{Rn}$  exposure system: once-through method.

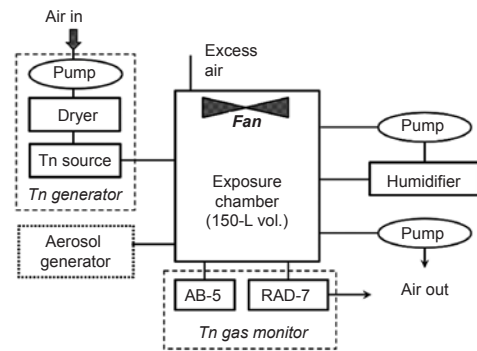


Fig. 3. Layout of  $^{220}\text{Rn}$  exposure system.

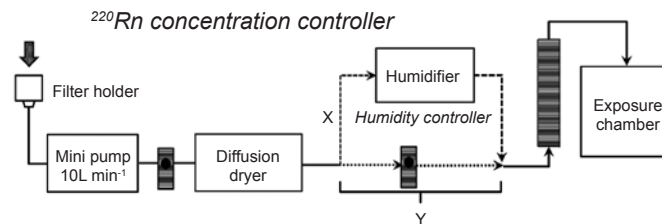


Fig. 4. Layout of X and Y directions in the  $^{220}\text{Rn}$  concentration controller section.

$$\lambda_e = (\lambda_{\text{Rn-222}} - \lambda_{\text{Po-214}}) \times (\lambda_{\text{Po-218}} - \lambda_{\text{Po-214}}) \times (\lambda_{\text{Pb-214}} - \lambda_{\text{Po-214}}) \times (\lambda_{\text{Bi-214}} - \lambda_{\text{Po-214}}) \quad (9)$$

### 2.1.2. Once-through method

The one-through method was designed to support experiments that require the use of aerosol particles in them. Figure 2 shows a schematic diagram of the whole system. After leaving uranium ore for one day in the acrylic container,  $^{222}\text{Rn}$  gas is injected by a pump into the mixing chamber. In this case, the  $^{222}\text{Rn}$  gas concentration can be controlled by the flow rate between the acrylic source container and the mixing chamber. The  $^{222}\text{Rn}$  gas is mixed with aerosol particles inside the chamber that are produced by a NaCl solution using an aerosol generator before being transferred to a 540 L exposure chamber made from acrylic plates for radiation instrument calibration and performance tests.

In this study, the first experiment was focused on the performance for stabilizing the  $^{222}\text{Rn}$  gas in the mixing chamber to maintain the concentration level.  $^{222}\text{Rn}$  was directly passed from an acrylic container into the mixing chamber via a polyethylene tube using a pump at different flow rates of 1, 5, and 10 L min<sup>-1</sup> for measuring the  $^{222}\text{Rn}$  concentration. An AB-5 monitor was used to continuously measure the count rate in the experiment every 10 seconds, for a period of 2 days. The temperature of the whole system was set by the temperature controller in the laboratory at 20 ± 2 °C, while the relative humidity (RH) was left unmodified. The  $^{222}\text{Rn}$

concentration in the chamber was estimated using the *CF* values similar to the spot-injection method.

### 2.2. Structure of $^{220}\text{Rn}$ exposure system

The layout of the  $^{220}\text{Rn}$  exposure system is shown in Figure 3. The system has three sections consisting of: a  $^{220}\text{Rn}$  concentration controller,  $^{220}\text{Rn}$  gas monitors, and an aerosol generator. The first step was aimed at maintaining the concentration level of  $^{220}\text{Rn}$  in the mixing chamber, which included the  $^{220}\text{Rn}$  concentration controller and the  $^{220}\text{Rn}$  gas monitors. Commercial lantern mantles (M-7910, Captain Stag, Japan) were used as the  $^{220}\text{Rn}$  and approximately 60 lantern mantles were stacked together in a 500 mL polycarbonate cylinder (6.7 cm diameter and 28.9 cm height) using wire screens (~6.5 cm diameter) according to the literature.<sup>13)</sup> and the total weight of the dry source with the cylinder was around 673.6 g. The source cylinder would be dried every time before use. The concentrations were controlled using different flow rates from X and Y directions (Fig. 4), which depended on the humidity level before and after passing into the  $^{220}\text{Rn}$  source cylinder. The total flow rate was set at 10 L min<sup>-1</sup> before dividing into two directions. Three conditions were prescribed by adjusting the flow rates from 0–6 L min<sup>-1</sup> using a mini pump.  $^{220}\text{Rn}$  concentration level varies with humidity and a high humidity is necessary to reduce the time needed to get the constant concentration, which is important for efficiency of calibration work. The value of relative humidity obtained after passing into the  $^{220}\text{Rn}$

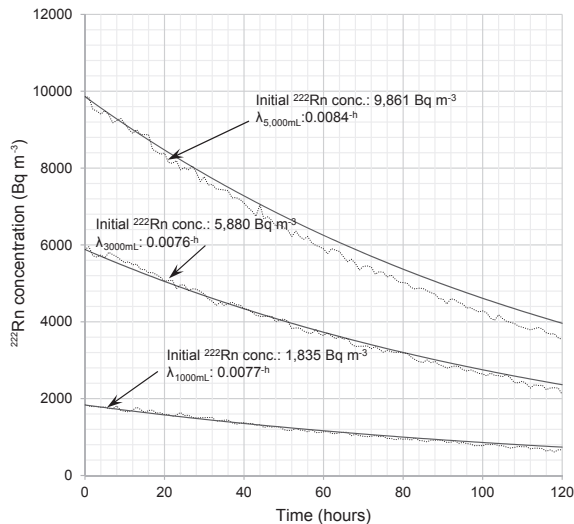


**Fig. 5.** Behavior of  $^{222}\text{Rn}$  decay in the exposure chamber for passive  $^{222}\text{Rn}$  monitor calibrations by spot-injection method and its decay constant compared with the decay constant calculated at  $0.0075\text{h}^{-1}$ .

column depended on the flow rate in the X direction. During  $^{220}\text{Rn}$  generation, the air from outside was filtered through a 47mm diameter glass microfiber filter (Whatman, England), mounted on a filter holder to purify it. Fresh air passed through five columns in a diffusion dryer until the relative humidity became low ( $<10\%$ ) before passing through a humidifier zone to control the humidity level.  $^{220}\text{Rn}$  gas from the source container was routed into the mixing chamber via a polyethylene tube.

In the second section, two  $^{220}\text{Rn}$  gas monitors were connected to the mixing chamber to monitor the level of  $^{220}\text{Rn}$  concentration there. An electrostatic collection radon/thoron monitor (RAD7, DurrIDGE. Co., Inc., USA) was installed to continuously measure the  $^{220}\text{Rn}$  concentration every 30 minutes. A grab sampling technique using the 300A scintillation cell with the AB-5 monitor was used for estimating the exact  $^{220}\text{Rn}$  concentration and the  $CF$  value in each condition, which was evaluated by the ratio between the  $^{220}\text{Rn}$  concentration obtained from the AB-5 monitor and the RAD7 monitor in  $\text{Bq m}^{-3}$  unit. Because of the short half-life of  $^{220}\text{Rn}$ , the data obtained by the RAD7 needed to be corrected in a calculation using the  $CF$  value.

This mixing chamber also supports addition of aerosol particles via an aerosol generator. However, the system was not set up with an aerosol generator as the condition was determined to be aerosol-free and it was not connected with the exposure chamber as this study focused on the performance tests and the stability of  $^{220}\text{Rn}$  concentration level. The system temperature was room temperature, around  $20 \pm 2^\circ\text{C}$ . In this case, the RH in the mixing chamber depended on the RH of the air after passed into the source container.

### 3. Results and discussion

#### 3.1. Reproducibility testing for released $^{222}\text{Rn}$ gas

The released  $^{222}\text{Rn}$  gas concentration was estimated 10 times using the spot-injection method to get the average value ( $n = 10$ ) of initial activity. The uranium ore was left undisturbed in the acrylic container for 1 day before injecting 2,000 mL of  $^{222}\text{Rn}$  gas into the chamber and then it was left for another day. The average initial activity value ( $\pm$  standard uncertainty) was evaluated to be approximately  $4,928 \pm 147 \text{ Bq m}^{-3}$ .

#### 3.2. $^{222}\text{Rn}$ concentration and stability of $^{222}\text{Rn}$ exposure system by spot-injection method

Three different volumes of  $^{222}\text{Rn}$  gas were measured every one hour. The counts obtained by the AB-5 monitor were converted to concentration ( $\text{Bq m}^{-3}$  unit) using the  $CF$  that was given by the Bateman equation<sup>18)</sup>. Behavior of  $^{222}\text{Rn}$  gas decay in the mixing chamber is shown in Figure 5. The decay constants in the experiments ( $\pm$  standard uncertainty) were estimated to be  $0.0077 \pm 0.00013 \text{ h}^{-1}$ ,  $0.0076 \pm 0.00020 \text{ h}^{-1}$ , and  $0.0084 \pm 0.00011 \text{ h}^{-1}$  for  $^{222}\text{Rn}$  gas injections at 1,000 mL, 3,000 mL, and 5,000 mL, respectively. The decay constants for the 1,000 mL and 3,000 mL conditions obtained were close to the value of  $0.0075 \text{ h}^{-1}$  calculated from half-life of  $^{222}\text{Rn}$  at 91.2 hours. For the 5,000 mL condition, the calculated value was about 13% higher and that might possibly be due to deterioration of the rubber materials in the joints as time passed, causing leakage of radioactive gases from the tank. The results indicated that there were no  $^{222}\text{Rn}$  gas leaks from the chamber during operation for the first two conditions and it should be possible to control the leakage of the gases in future work. The concentration obtained was found between 0.2 and  $10 \text{ kBq m}^{-3}$ . The method developed in this study can be used for  $^{222}\text{Rn}$  gas monitors by calculating time-integrated  $^{222}\text{Rn}$  concentration. However, this method is used only for calibration without aerosol generation.

#### 3.3. $^{222}\text{Rn}$ concentration and stability of $^{222}\text{Rn}$ exposure system by once-through method

In order to study the stability of  $^{222}\text{Rn}$  concentration using the once-through method, three different flow rates were chosen for maintaining the  $^{222}\text{Rn}$  concentration levels. The  $^{222}\text{Rn}$  concentration in the beginning was found to be the highest level during the operation and gradually fell as it reached the equilibrium state (Fig. 6). The amount of time from the first phase (at the beginning) until it reached equilibrium depended on the adjusted flow rate from the source-container into the exposure chamber. In time until the equilibrium state was obtained was found to be approximately 5, 7, and 9 hours for 1, 5, and  $10 \text{ L min}^{-1}$  conditions, respectively. The concentration was measured

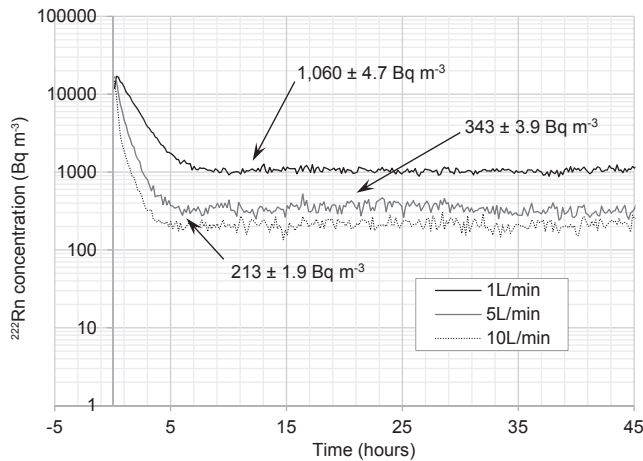


**Fig. 6.** Relationship between  $^{222}\text{Rn}$  concentrations ( $\pm$  standard uncertainty) and flow rates by once-through method.

every 10 minutes and converted to the corrected values by the  $CF$ s as shown in Table 3. Figure 6 shows the average concentrations for the equilibrium state in each condition.

The results indicated that the flow rate is an important factor for controlling the  $^{222}\text{Rn}$  concentration level in the system. As the limit of  $^{222}\text{Rn}$  emanated varies based on the releasing rate of  $^{222}\text{Rn}$  gas from the uranium ore, lowering the flow rate from the source container resulted in increased concentration, while raising the flow rate decreased the concentration. Currently, this system can set the concentration level to be between 200 to 1,000  $\text{Bq m}^{-3}$ .

Additionally, any  $^{222}\text{Rn}$  gas in the last 10 hours should be removed before starting operation of the exposure system, as shown in the concentration graphs in Fig. 6 for calibrating the radioactive gas monitors. In order to maintain stability of the  $^{222}\text{Rn}$  concentration level, a valve should be installed in the system for switching the route of the gas when starting the injection into the chamber.

#### 3.4. $^{220}\text{Rn}$ concentration and stability of $^{220}\text{Rn}$ exposure system

Three flow rate conditions were carried out for testing the performance of the exposure system (Table 4). The concentration ( $C_{\text{Tn}}$ ) was estimated using the average value of  $CF$  ( $C_{\text{Tn-RAD7}}/C_{\text{Tn0}}$ ) from the initial  $^{220}\text{Rn}$  concentration ( $C_{\text{Tn0}}$ :  $\text{Bq m}^{-3}$ ) obtained by three grab samplings<sup>18)</sup> in each condition using the AB-5 monitor and multiplying it with the value obtained by the RAD7 ( $C_{\text{Tn-RAD7}}$ :  $\text{Bq m}^{-3}$ ) that was calculated according to equations (10) - (11).

$$C_{\text{Tn}} = C_{\text{Tn-RAD7}} \times F_t \times F_d \times CF \quad (10)$$

**Table 3.** The conversion factors for  $^{222}\text{Rn}$  concentration calculation in once through method

Time interval in hours	$\overline{CF}$ ( $\text{Bq m}^{-3} \text{cpm}^{-1}$ ) <sup>a</sup>
0 – 10	52.4
10 – 20	44.6
20 – 30	41.6
30 – 40	39.2
40 – 50	37.1
50 – 60	35.3
60 – 70	33.7
70 – 80	32.5
80 – 90	31.6
90 – 100	30.8
100 – 110	30.2
110 – 120	29.7
120 – 130	29.4
130 – 140	29.1
140 – 150	28.9
150 – 160	28.7
160 – 170	28.5
170 – 180	28.5
180 – 190	28.4
190 – 200	28.4
200 – 210	28.4
> 210	28.3

<sup>a</sup> $\overline{CF}$  is defined as a time interval during measurements

$$C_{\text{Tn0}} = \frac{C_1 - kC_2}{V \times (\eta_{\text{Rn-220}} + \eta_{\text{Po-216}}) \int_{t_0}^{t_0+t_m} e^{-\lambda_{\text{Rn}} t} dt} \quad (11)$$

Here, where  $F_t$  is the correction factor for decay compensation while the gas is flowing in the polyethylene tube from the chamber to the dryer before entering the RAD7, which in this study was 0.923.  $F_d$  is the correction factor for decay compensation while the gas is flowing through the dryer (=2).  $C_1$  is counts in the first measurement period.  $C_2$  is counts in the second measurement period.  $k$  is the constant of the ratio between  $^{222}\text{Rn}$  and its progeny in the cell that can be approximately assigned as 0.2.  $V$  is the inner volume of the cell ( $0.00027 \text{ m}^3$ ). Alpha counting efficiencies of the scintillation cell were estimated by a Monte Carlo calculation at 0.736 for  $\eta_{\text{Rn-220}}$  and 0.780 for  $\eta_{\text{Po-216}}$ . The beginning time of the measurement ( $t_0$ : s) was given as 20 s, and the measurement period ( $t_m$ : unit of s) was given as  $100 \text{ s}^{18)}$ .

The  $CF$  values were estimated to be 1.04, 1.09, and 0.99 for Case I, Case II, and Case III, respectively. Table 4 shows all flow rate conditions, the average concentration values, temperature, RH, and the absolute humidity (AH) after passing the  $^{220}\text{Rn}$  source column. Weight of water in the source cylinder was estimated to calculate the AH value by weighting dried lantern mantles with the

**Table 4.** The relationship between the flow rate X and Y directions, the average values of  $^{220}\text{Rn}$  concentration obtained from  $^{220}\text{Rn}$  exposure system ( $C_{\text{Tn}}$ ), % relative humidity (%RH), temperature (T), and absolute humidity (AH)

	X L min <sup>-1</sup>	Y L min <sup>-1</sup>	CTna (kBq m <sup>-3</sup> )	%RH <sup>a, b</sup>	T <sup>a</sup> (°C)	AH <sup>a, c</sup> (g m <sup>-3</sup> )
Case I	0	10	3.5 ± 0.03	11 ± 0.1	13 ± 0.04	1.2 ± 0.01
Case II	4	6	9.2 ± 0.04	39 ± 0.1	15 ± 0.06	5.0 ± 0.02
Case III	6	4	29.0 ± 0.10	61 ± 0.1	14 ± 0.05	7.3 ± 0.02

<sup>a</sup>Arithmetic mean ± standard uncertainty

<sup>b</sup>%RH value obtained after passing  $^{220}\text{Rn}$  source

<sup>c</sup>AH value obtained after passing  $^{220}\text{Rn}$  source

cylindrical container (total weight: 673.6 g) before testing. Total weight of the source cylinder from Case II and Case III increased from the dry weight to 678 g (0.65%) and 680.9 g (1.08%), respectively.

The water vapor concentration in the air from the  $^{220}\text{Rn}$  generation directly affected the increase of  $^{220}\text{Rn}$  concentration as the total weight of the source container increased exponentially with increasing AH. High AH resulted in high  $^{220}\text{Rn}$  concentration in the system, while low AH caused a decrease in  $^{220}\text{Rn}$  production<sup>13</sup>. In comparison, the results of the experiment were somewhat similar to those derived from the previous report<sup>13</sup>. The influence of the moisture content has been demonstrated by the emanation processes in several studies<sup>13, 19</sup>, in which the phenomenon of lower recoil range in water than in air has been explained for a  $^{220}\text{Rn}$  atom. A  $^{220}\text{Rn}$  atom that enters a pore space filled with water, will be terminated its recoil in the water and then transfer  $^{220}\text{Rn}$  into the air<sup>13</sup>. Therefore, humidity from water can explain the relationship between the increase in  $^{220}\text{Rn}$  concentration and AH. The average AH values were estimated as 1.2 g m<sup>-3</sup> to 7.3 g m<sup>-3</sup> and AH was released to the concentration directly. Likewise, Hosoda *et al.*<sup>20</sup> reported that the effects of moisture can increase  $^{220}\text{Rn}$  concentration. After passing different absolute humidity into a soil sample, they found the concentration level increased about 2.4 times while the absolute humidity increased from 1.4 g cm<sup>-3</sup> to 17.5 g cm<sup>-3</sup>, which is similar to the finding of this study. In addition, they also observed that the influences of hysteresis affected the increase and decrease of  $^{220}\text{Rn}$  concentration level.

In summary, the results obtained indicated that this exposure system could be used for  $^{220}\text{Rn}$  gas monitor calibrations. The  $^{220}\text{Rn}$  exposure system could set the concentration from 3,500 to 30,000 Bq m<sup>-3</sup> (Fig. 7) and stability was obtained after 10 and 20 hours for Case II and Case III, respectively, and in Case I the concentration stability was obtained in the first hour. However, to be able to perform calibration work efficiently, the time between the starting point and the constant state should be as short as possible, and that could be reduced by increasing the moisture of the source container before use.

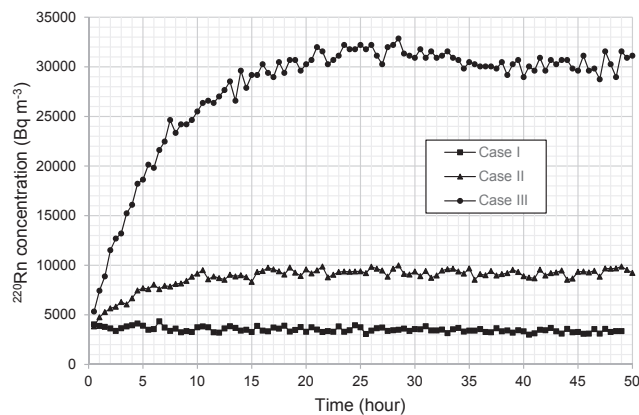


**Fig. 7.** Relationship between  $^{220}\text{Rn}$  concentrations and humidity in the  $^{220}\text{Rn}$  exposure system: Case I shows stability of  $^{220}\text{Rn}$  concentration at humidity 11%; X direction at the flow rate 0 L min<sup>-1</sup> and Y direction at the flow rate 10 L min<sup>-1</sup>. Case II shows stability of  $^{220}\text{Rn}$  concentration at humidity 39%; X direction at the flow rate 4 L min<sup>-1</sup> and Y direction at the flow rate 6 L min<sup>-1</sup>. Case III shows stability of  $^{220}\text{Rn}$  concentration at humidity 61%; X direction at the flow rate 6 L min<sup>-1</sup> and Y direction at the flow rate 4 L min<sup>-1</sup>.

#### 4. Conclusion

The results obtained from this study indicated that both systems could be easily controlled by manually setting the flow rate and relative humidity, and the desired concentration levels could be maintained during operation. For the  $^{222}\text{Rn}$  exposure system, the concentration level depended on the volume of gas for the spot-injection method and flow rate of the radioactive gas during operation affected  $^{222}\text{Rn}$  concentration level in the once-through method, whereas the relative humidity affected the  $^{220}\text{Rn}$  concentration level for the  $^{220}\text{Rn}$  exposure system. The concentration of  $^{220}\text{Rn}$  could be controlled by reducing or increasing the level of moisture through the  $^{220}\text{Rn}$  source column. Currently, the  $^{222}\text{Rn}$  exposure system can set the concentration level to be between 0.2 and 10 kBq m<sup>-3</sup> due to restrictions on the radiation sources, which are limited by the releasing rate. The  $^{220}\text{Rn}$  concentration level for this system could be set between 3.5 and 29 kBq m<sup>-3</sup> based on moisture content of the  $^{220}\text{Rn}$  source. Additionally, the types of sources, flow rates of

the radioactive gases generated into the chamber, gases emanating from the sources and humidity in the gas generation system are important factors affecting for the range of  $^{222}\text{Rn}$ - $^{220}\text{Rn}$  concentration levels. In the future, this  $^{222}\text{Rn}$  exposure system can be used for testing the performance of  $^{222}\text{Rn}$ ,  $^{220}\text{Rn}$  and their progeny monitors and calibration of other monitors.

## 5. Conflict of Interest Disclosure

The authors declare that they have no conflict of interest

## References

1. WHO. WHO handbook on indoor radon: a public health perspective. WHO. Geneva; 2009.
2. WHO [Internet]. Geneva: WHO. Environmental radiation. [cited 2016 Feb 18]. Available from: [http://www.who.int/ionizing\\_radiation/env/en/](http://www.who.int/ionizing_radiation/env/en/)
3. UNSCEAR. UNSCEAR 2000 REPORT Vol. II: Sources and effects of ionizing radiation. United Nations Scientific Committee on the Effects of Atomic Radiation. New York: United Nations; 2000.
4. EPA. [Internet]. Washington, D.C.: EPA; 2013 [cited 2016 July 19]. Basic radon facts. Available from: <https://www.epa.gov/radon/basic-radon-facts> Accessed 19 July 2016
5. Zhao C, Zhuo W, Chen B and Zhang H. Characteristic and performance of a sample thoron chamber. *Radiat Prot Dosim.* 2010;141(4):444–7.
6. Steinhäusler F. Environmental  $^{220}\text{Rn}$ : a review. *Environ Int.* 1996;22(Suppl. 1):S1111–S1123.
7. Nuccetelli C and Bochicchio F. The thoron issue: monitoring activities, measuring techniques and dose conversion factors. *Radiat Prot Dosim.* 1998;78:59–64.
8. Doi M and Kobayashi S. Characterization of Japanese wooden houses with enhanced radon and thoron concentrations. *Health Phys.* 1994;66:274–82.
9. Shang B, Chen B, Gao Y, Wang Y, Cui H. and Li Z. Thoron levels in traditional Chinese residential dwellings. *Radiat Environ Biophys.* 2005;44:193–9.
10. Kim YJ, Lee HY, Kim CS, Chang BU, Rho BH, Kim CK and Tokonami S. Indoor radon, thoron and thoron daughters concentrations in Korea. High levels of natural radiation and radon areas: Radiation dose and health effects. *Int Congr Ser.* 2005;1276:46–9.
11. Ichitsubo H, Yamada Y, Shimo M and Koizumi A. Development of a radon-aerosol chamber at NIRS-general design and aerosol performance. *Aerosol Sci Technol.* 2004;35:217–32.
12. Janik M, Tokonami S, Kovács T, Kávási A, Kranrod C, Sorimachi A, et al. International intercomparisons of integrating radon detectors in the NIRS radon chamber. *Appl Radiat Isot.* 2009;67:1691–6.
13. Sorimachi A, Ishikawa T, Janik M, Tokonami S. Quality assurance and quality control for thoron measurement at NIRS. *Radiat Prot Dosim.* 2010;141(4):367–70.
14. Shweikani R, Raja G. Design, construct and test of a calibration radon chamber. *Radiat Meas.* 2005;40:316–9.
15. Al-Azmi D. The use of soil gas as radon source in radon chambers. *Radiat Meas.* 2009;44:306–10.
16. Abdalla A M, Al-Hajry A. Radon irradiation chamber and its applications. *Nucl Instrum Meth A.* 2015;786:78–82.
17. Bogacz J, Mazur J, Swakoń J, Janik M. The calibration of activated charcoal detectors in a small  $^{222}\text{Rn}$  exposure chamber. *Radiat Meas.* 2001;33:873–8.
18. Tokonami S, Yang M, Yonehara H, Yamada Y. Simple, discriminative measurement technique for radon and thoron concentrations with a single scintillation cell. *Rev Sci Instrum.* 2002;73:69.
19. Nazaroff WW, Nero AV. Radon and its decay products in indoor air. New York: Wiley;1988.
20. Hosoda M, Sorimachi A, Tokonami S, Ishikawa T, Sahoo S K, Hassan N M M, et al. Generation and control of radon from soil. Proceedings of the 12<sup>th</sup> Congress of the International Radiation Protection Association [Internet]. 2010 [cited 2016 July 19]. Available from: [http://www-pub.iaea.org/MTCD/Publications/PDF/P1460\\_Comp\\_CD/Start.pdf](http://www-pub.iaea.org/MTCD/Publications/PDF/P1460_Comp_CD/Start.pdf)